

Strain tuned magnetoelectric coupling in orthorhombic Y Mn O 3 thin films

X. Marti, I. Fina, V. Skumryev, C. Ferrater, M. Varela, L. Fábrega, F. Sánchez, and J. Fontcuberta

Citation: *Applied Physics Letters* **95**, 142903 (2009); doi: 10.1063/1.3238287

View online: <http://dx.doi.org/10.1063/1.3238287>

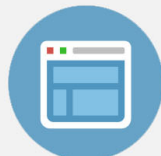
View Table of Contents: <http://scitation.aip.org/content/aip/journal/apl/95/14?ver=pdfcov>

Published by the [AIP Publishing](#)



Re-register for Table of Content Alerts

Create a profile.



Sign up today!



Strain tuned magnetoelectric coupling in orthorhombic YMnO_3 thin films

X. Marti,^{1,a)} I. Fina,¹ V. Skumryev,² C. Ferrater,³ M. Varela,³ L. Fábrega,¹ F. Sánchez,¹ and J. Fontcuberta¹

¹Institut de Ciència de Materials de Barcelona (ICMAB-CSIC), Campus UAB, 08193 Bellaterra, Spain

²Departamento Física, Universitat Autònoma de Barcelona (UAB), Campus UAB, 08193 Bellaterra,

Spain and Institut Català de Recerca i Estudis Avançats, Lluís Companys 23, 08010 Barcelona, Spain

³FAO and IN2UB, Universitat de Barcelona, Diagonal 647, 08028 Barcelona, Spain

(Received 31 July 2009; accepted 7 September 2009; published online 5 October 2009)

Orthorhombic YMnO_3 epitaxial thin films were grown on Nb(0.5%)-doped $\text{SrTiO}_3(001)$ substrates. Film's thickness was varied to tune the epitaxial strain. Structural and magnetic properties are well correlated, presenting a more pronounced ferromagnetic behavior as the unit cell becomes more distorted. Dielectric properties were investigated as a function of the temperature and magnetic field. The dielectric peak occurring at temperatures below the antiferromagnetic ordering is proved to be magnetoelectric and its amplitude is dependent on the unit cell distortion. These findings allow tailoring ferromagnetic and magnetoelectric properties via epitaxial strain. © 2009 American Institute of Physics. [doi:10.1063/1.3238287]

Magnetoelectric materials are being investigated as they can provide a shortcut to the transduction from electric (magnetic) to magnetic (electric) properties. The search for materials displaying such features and the physical mechanism involved has triggered an intense research. Particularly relevant is the recent discovery that pronounced dielectric anomalies or even ferroelectricity can be obtained, in the so-called improper ferroelectrics, subsequent to magnetic ordering (see, for instance Ref. 1).

Orthorhombic rare earth manganites (RMnO_3) have become one of the most studied materials of such systems. On one hand, they all present antiferromagnetic ordering of the Mn moments with a complex magnetic phase diagram. At low temperatures, depending on the Mn–O–Mn bonding angle, different magnetic structures are found: *A*-type, spiral, or *E*-type.² As temperature increases, above the so-called lock-in temperature (T_L), an antiferromagnetic incommensurate phase appears up to the Néel temperature (T_N) where the materials become paramagnetic. On the other hand, the non-collinear order in spiral magnets^{2–4} or nonsymmetrical magnetic striction in *E*-type antiferromagnets⁵ provide mechanisms to obtain ferroelectricity. It follows that the dielectric properties (linked to the charge distribution in the orbitals) arising from magnetic order must be sensitive to magnetic fields and strongly anisotropic. Indeed, magnetic field dependent ferroelectricity and permittivity anomalies have been reported for all the spiral structures in single crystals² and for polycrystalline *E*-type^{6,7} bulk RMnO_3 .

In contrast, the dielectric properties of orthorhombic RMnO_3 thin films have been scarcely reported.^{8–10} Besides, the unexpected observation of ferromagnetism in thin films, otherwise antiferromagnetic in bulk, has focussed more attention.^{8,9,11–14} Our recent results on orthorhombic YMnO_3 indicate that the ferromagnetic behavior increases with the unit cell distortion.¹⁴ However, the analysis of the impact of the lattice distortion on the dielectric properties in thin films has remained unrevealed.

Here we report on the dielectric properties of orthorhombic epitaxial YMnO_3 thin films. Since Y^{3+} is nonmagnetic, it allows to discriminate the magnetoelectric effects due to the Mn sublattice. We will first discuss the dielectric permittivity as a function of the temperature. A peak is found below T_N and its location depends on the magnetic field, suggesting a magnetoelectric coupling. At a constant temperature, dielectric permittivity presents a $\varepsilon \sim \alpha M^2$ behavior and the α coefficient increases as the unit cell distortion decreases. The findings allow identifying the conditions where ferromagnetism and dielectric permittivity anomalies coexist and can be simultaneously exploited.

Thin films were deposited by pulsed laser deposition on (001)-oriented 0.5%-Nb: SrTiO_3 substrates at 785 °C, 0.3 mbar of oxygen pressure and at a growth rate of 0.13 Å/pulse. Crystal structure was investigated using 4-circle x-ray Philips' diffractometer. Magnetic data were recorded using a Quantum Design super conducting quantum interference device with the magnetic field applied perpendicular to the sample. Capacitance measurements were carried out at 100 mV and at 100 kHz using an LF4182 impedance analyzer (Agilent Co.). Pt top electrodes (0.25 mm²) were deposited *ex situ*. The electric field was applied perpendicular to the film.

$\theta/2\theta$ and reciprocal space maps (not shown here) indicate that all films are orthorhombic, epitaxial, and (001)-oriented according to the *Pbnm* setting. We shall discuss a set of four thin films with thicknesses: 14, 28, 64, and 134 nm. The unit cell is shrunk in the thinnest films whereas it gradually relaxes toward the bulk dimensions as the thickness increases. Additional structural details can be found elsewhere.^{14,15}

Figure 1(a) (circle symbols) shows the temperature dependence of the zero-field cooled/field cooled (ZFC-FC) magnetization measured for the thickest and most relaxed film at 500 Oe. The observed splitting in the ZFC-FC curves reveals the existence of remanent magnetization below $T_N \sim 50$ K. Simultaneously, its dielectric permittivity (diamond symbols) displays a gradual increase reaching at $T_g \sim 20$ K a maximum change of up to 22% [calculated as $\Delta\varepsilon = [\varepsilon(T) - \varepsilon(60 \text{ K})] / \varepsilon(60 \text{ K})$]. These results are in close

^{a)}Electronic mail: xavi.mr@gmail.com.

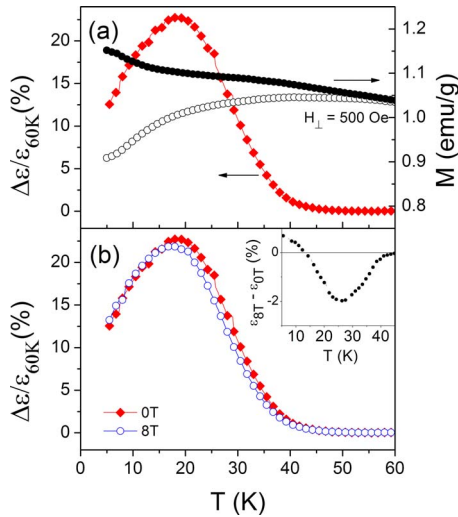


FIG. 1. (Color online) (a) Temperature dependence of the ϵ normalized at its value at 60 K (left axis) and ZFC and FC magnetization (right axis) for the 134 nm thick film. (b) ϵ measured at zero magnetic field (solid symbols) and at 8 T (empty symbols). Inset: subtraction of both curves.

correspondence with previous YMnO_3 reports in both bulk⁶ and thin films,⁸ and with other reported RMnO_3 .^{2,7} Therein, the ϵ peak was attributed to the emergence of ferroelectricity after the establishment of the spiral or E -type antiferromagnetic order. Since the magnetic structure of YMnO_3 (Ref. 16) is the result of a competition of interactions where the spins are modulated along the $[010]$ direction, it can be expected that a magnetic field would alter such subtle equilibrium and modify the lock-in temperature. Indeed, previous work on single crystals² of the related compounds TbMnO_3 and DyMnO_3 reported a shift toward lower temperatures of the dielectric peak when a magnetic field was applied along the c axis. It was proposed² that the magnetic field favors the in-plane ferromagnetic interactions, thus decreasing T_L . Therefore, the shift of the dielectric peak under magnetic field indicates magnetoelectric coupling. Data in Fig. 1(b) follows such behavior: when the temperature dependence of ϵ is measured with 8 T applied along the c axis (empty symbols), the ϵ peak is shifted to lower temperatures with respect to the initial curve (solid symbols). Subtraction of the permittivity curves with and without magnetic field is shown in the inset. The data show that the changes are maxima at $T_{\Delta\epsilon} \sim 25$ K, displaying a reduction of up to 2%.

To further investigate its magnetoelectric nature, we measured the dielectric permittivity as we cycled the magnetic field at $T_{\Delta\epsilon}$ along the c direction. The data corresponding to the sample discussed in Fig. 1 are shown in Fig. 2(b). Firstly, the data show a decrease of up to 2% in $\epsilon(H)$, irrespective of the sign of the applied magnetic field. The small hysteresis of less than 0.2% will be discussed later. Similar dependencies of $\epsilon(H)$ are obtained in all measured films in the set of samples with different thicknesses (not shown here). The corresponding magnetization loop is shown in Fig. 2(a). Substrate contribution was removed. The loop presents a linear response with the magnetic field at high magnetic fields as expected for an antiferromagnet. The hysteresis in the low field region (inset) corresponds to the ZFC-FC splitting observed in Fig. 1(a) and will be discussed afterwards. According to neutron diffraction data,¹⁶ Mn magnetic moments are arranged collinearly along the $[010]$ direction, which in our samples is contained in-plane of the

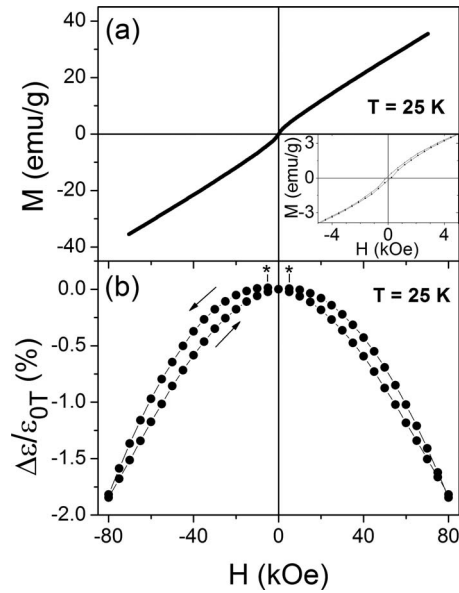


FIG. 2. (a) Magnetization loop at 25 K. Inset: zoom of the curve. (b) Change in the ϵ at 25 K with the magnetic field. Arrows indicate how the magnetic field is cycled. Asterisks signal the maxima in the $\epsilon(H)$ curves.

sample. When the magnetic field is applied perpendicular to the spin axis of an antiferromagnet, the measured magnetization corresponds to the field-induced tilting of the spins with respect to the zero magnetic field positions. A comparison of both panels in Fig. 2 shows that at $T_{\Delta\epsilon} \sim 25$ K as the tilt of the spins becomes larger, the electrical permittivity is reduced.

It follows that there is a connection between the magnetic state (i.e., field-induced tilting of the spins) and the electrical permittivity. Starting from a phenomenological Ginzburg–Landau model,² it is reported that at temperatures close to the magnetic transition, the change in the dielectric permittivity should behave as $\epsilon \sim \alpha M^2$, where α is the magnetoelectric coupling coefficient. Illustrative examples of this M^2 dependence have been previously reported for ϵ - Fe_2O_3 nanoparticles¹⁷ and multiferroic BiMnO_3 samples.² Figure 3(a) shows the mentioned plot for our set of samples. A linear dependence is observed for all samples, indicating that ϵ is determined by the magnetization and, hence, by the field-induced tilting. We now focus on the different slopes which are obtained for each film depending on its thickness. Since the magnetic structure is highly dependent on the unit cell topology and the dielectric properties arise from the magnetic order, the epitaxial strain appears as a natural method to tune both the magnetic and dielectric properties. Indeed, data in Fig. 3(b) indicate that the magnetoelectric coupling can be controlled via the unit cell distortion. It turns out that the more the distorted unit cell, the less magneto-

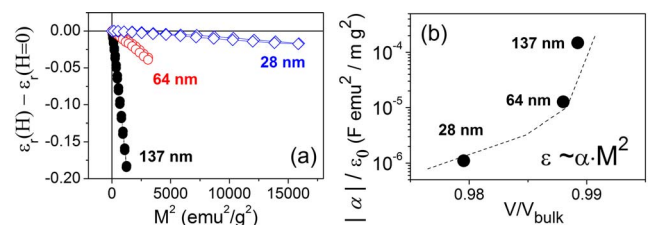


FIG. 3. (Color online) (a) Relative dielectric permittivity as a function of M^2 for samples with different thicknesses. Plots are shifted by the ϵ_r at 0 T. (b) Magnetoelectric coefficient versus unit cell distortion.

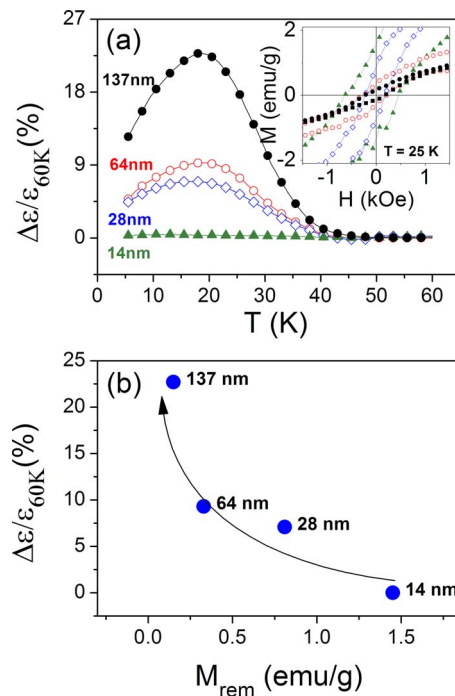


FIG. 4. (Color online) (a) Temperature change in the dielectric permittivity relative to its value at 60 K for samples with different thicknesses. Inset: remanent magnetization at 25 K. (b) Relative change of ϵ as a function of the remanent magnetization.

electric coupling. In fact, the sample presenting the most distorted unit cell (14 nm thick) did not present any measurable dependence of the ϵ with the magnetic field.

We now present an approach to investigate the role of the spins collinearity into the dielectric properties. The ferromagnetism observed in Figs. 1(a) and 2(a) increases as the unit cell is more distorted¹⁴ and can be described as a strain-induced canting of the Mn magnetic moment.^{11,14} Therefore, even in the absence of magnetic field, the spontaneous non-collinear magnetic order is expected to resound in the dielectric properties. Fig. 4 shows the spontaneous magnetization (inset) and the temperature dependence of ϵ (main panel) at the magnetic transition. Figure 4(b) shows that as the remanent magnetization increases, the amplitude of the dielectric peak decreases. It is, the more collinear the spins are arranged, the larger increase in the ϵ . Current models for ferroelectricity in antiferromagnetic systems propose that electric polarization arises from tiny atomic displacements due to anisotropic exchange interactions or magnetic striction.³⁻⁵ Within this context, it seems plausible that, as the spins become more correlated as ferromagnetism arises, the dielectric polarizability and thus ϵ would be reduced. On the other hand, larger electrical dipoles are predicted as the non-collinearity of the spins increases.^{3,4} Being that so, larger electrical dipoles would be present in the most ferromagnetic films and, in the frame of simple ferroelectric models, a decrease in the electrical permittivity would be expected.

Finally, we address the hysteresis in both the magnetization and ϵ curves displayed in Fig. 2. On one hand, detailed inspection of the inset in Fig. 2 shows that the magnetization loop is hysteretic below 5000 Oe. In the previous paragraph, we have shown that the ϵ depends on the field-induced tilting of the spins. On this ground, it could be expected that the

magnetic hysteresis would be reflected in the dielectric properties. Indeed, it is worth noting that the maxima in the ϵ curves (signaled by asterisks) are intriguingly located at 5000 Oe, at the onset of magnetic hysteresis. On the other hand, $\epsilon(H)$ present an small hysteresis at least up to 80 kOe. Its contribution ($\sim 0.2\%$) is at least one order of magnitude smaller than the total change induced by magnetic field ($\sim 2\%$). Its origin cannot be determined within the present experiments, but would it be compatible with an eventual ferroelectric character of the thin films.

In summary, we have shown that an increase of up to 22% in the dielectric constant occurs below the Néel temperature in epitaxial orthorhombic YMnO₃ thin films. The dielectric peak depends on the external magnetic field, indicating magnetolectric coupling. Dielectric permittivity is found to follow a $\epsilon \sim \alpha M^2$ dependence. The magnetolectric coefficient depends on the unit cell topology, being larger for the less distorted unit cells. Dielectric characterization at zero magnetic field of differently canted structures confirms that the permittivity is related to the tilting of the spins. The findings provide a path to tune the magnetolectric coupling via epitaxial strain and, at the same time, obtain ferromagnetic films with magnetodielectric coupling.

Financial support by the Spanish Government (Project Nos. MAT2008-06761-C03 and NANOSELECT CSD2007-00041) and by EU [Project MaCoMuFi (No. FP6-03321)] is acknowledged.

¹D. Khomskii, *Phys.* **2**, 20 (2009).

²T. Kimura, S. Kawamoto, I. Yamada, M. Azuma, M. Takano, and Y. Tokura, *Phys. Rev. B* **67**, 180401 (2003).

³H. Katsura, N. Nagaosa, and A. V. Balatsky, *Phys. Rev. Lett.* **95**, 057205 (2005).

⁴M. Mostovoy, *Phys. Rev. Lett.* **96**, 067601 (2006).

⁵I. A. Sergienko, C. Sen, and E. Dagotto, *Phys. Rev. Lett.* **97**, 227204 (2006).

⁶B. Lorenz, Y. Q. Wang, Y. Y. Sun, and C. W. Chu, *Phys. Rev. B* **70**, 212412 (2004).

⁷B. Lorenz, Y.-Q. Wang, and C. W. Chu, *Phys. Rev. B* **76**, 104405 (2007).

⁸X. Marti, V. Skumryev, V. Laukhin, F. Sánchez, M. V. García-Cuenca, C. Ferrater, and M. Varela, *J. Mater. Res.* **22**, 2096 (2007).

⁹D. Rubi, S. Venkatesan, B. J. Kooi, J. Th. M. De Hosson, T. T. M. Palstra, and B. Noheda, *Phys. Rev. B* **78**, 020408 (2008).

¹⁰T. H. Lin, H. C. Shih, C. C. Hsieh, C. W. Luo, J.-Y. Lin, J. L. Her, H. D. Yang, C.-H. Hsu, K. H. Wu, T. M. Uen, and J. Y. Juang, *J. Phys.: Condens. Matter* **21**, 026013 (2009); see also T. C. Han and J. G. Lin, *Appl. Phys. Lett.* **94**, 082502 (2009).

¹¹C. C. Hsieh, T. H. Lin, H. C. Shih, C.-H. Shu, C. W. Luo, L.-Y. Lin, K. H. Wu, T. M. Uen, and J. Y. Juang, *J. Appl. Phys.* **104**, 103902 (2008).

¹²B. J. Kirby, D. Kan, A. Luykx, M. Murakami, D. Kundaliya, and I. Takeuchi, *J. Appl. Phys.* **105**, 07D917 (2009).

¹³D. Rubi, C. de Graaf, C. J. M. Daumont, D. Mannix, R. Broer, and B. Noheda, *Phys. Rev. B* **79**, 014416 (2009).

¹⁴X. Marti, V. Skumryev, A. Cattoni, R. Bertacco, V. Laukhin, C. Ferrater, M. V. García-Cuenca, M. Varela, F. Sánchez, and J. Fontcuberta, *J. Magn. Mater.* **321**, 1719 (2009).

¹⁵X. Marti, F. Sánchez, V. Skumryev, V. Laukhin, C. Ferrater, M. V. García-Cuenca, M. Varela, and J. Fontcuberta, *Thin Solid Films* **516**, 4899 (2008).

¹⁶A. Muñoz, J. A. Alonso, M. T. Casais, M. J. Martínez-Lope, J. L. Martínez, and M. T. Fernández-Díaz, *J. Phys.: Condens. Matter* **14**, 3285 (2002).

¹⁷M. Gich, C. Frontera, A. Roig, J. Fontcuberta, E. Molins, N. Bellido, Ch. Simon, and C. Fleta, *Nanotechnology* **17**, 687 (2006).